Dalton Transactions

ROYAL SOCIETY OF CHEMISTRY

COMMUNICATION

View Article Online
View Journal

Cite this: DOI: 10.1039/d4dt02344g

Received 16th August 2024,
Accepted 3rd January 2025

DOI: 10.1039/d4dt02344g

rsc.li/dalton

Inorganic–organic hybrid nanoparticles with carbonate-triggered emission-colour-shift†

Christian Ritschel,[a] Lena J. Daumann [b] and Claus Feldmann [*a]

$(Eu^{3+}{}_4[PTC]^{4-}{}_3)_{0.78}(Eu^{3+}[TREN\text{-}1,2\text{-}HOPO]^{3-})_{0.22}$ inorganic–organic hybrid nanoparticles (IOH-NPs) contain Eu^{3+}, tris[(1-hydroxy-2-oxo-1,2-dihydropyridine-6-carboxamido)ethyl]amine (TREN-1,2-HOPO) and perylene-3,4,9,10-tetracarboxylate (PTC). The IOH-NPs are prepared in water and exhibit a rod-type shape, with a length of 60 nm and a diameter of 5 nm. Particle size and chemical composition are examined by different methods (SEM, DLS, FT-IR, TG, C/H/N analysis). With TREN-1,2-HOPO as antenna, the IOH-NPs show Eu^{3+}-based red emission, whereas the PTC emission is totally quenched due to π-stacking in the solid nanoparticles. After addition of carbonate, PTC is released from the IOH-NPs into solution, resulting in an increasing green emission of free PTC. The resulting carbonate-driven shift of the emission colour from red to green surprisingly allows to determine the carbonate concentration qualitatively and quantitatively in a concentration range of 1 μM to 2 mM and was tested for tap water as a specific example.

Introduction

Luminescence is an ideal tool for all kinds of sensing and monitoring as the detection is easy, cheap and non-invasive.[1] This includes sensing of specific atoms, ions, or molecules,[2] monitoring of biomolecules (*e.g.*, peptides, DNA, antibodies),[3] or optical imaging in biosciences (to study, *e.g.*, cellular uptake, cell functions, drug release).[4] Most often, optical detection is based on a change in intensity up to an on–off or off–on behaviour.[1–4] Luminescence detection *via* a change of the emission intensity, however, has the disadvantage to be concentration-dependent and requires a normalization of the emission intensity on a suitable reference or a distinct on–off/off–on characteristics. Less often, so-called ratiometric fluorescence sensing was used with a change of wavelength and emission colour, which can be more sensitive and independent from concentration.[5] Here, most often molecules and/or coordination complexes were described. In regard of nanoparticles, gold, quantum dots, metal–organic frameworks (MOFs), or carbon dots were used most often.[6]

Aiming at luminescence-based sensing, moreover, lanthanide (Ln)-based compounds are specifically interesting for detection due to their narrow line width.[7] Especially, Eu^{3+}-based complexes have been intensively studied to detect ions such as Zn^{2+},[8] Cu^{2+},[9] Hg^{2+},[10] F^-,[11] PO_4^{3-},[12] HCO_3^-/CO_3^{2-},[13] lactate,[14] *etc.* Here, a general restriction of f–f transitions on lanthanides relates to their sensitivity to quenching in the presence of water/moisture due to non-luminescent relaxation *via* O–H vibrations.[15] In addition to molecular species, nanoparticles offer further advantages for luminescence detection as they can show size-dependent emission (*e.g.*, quantum dots, carbon dots)[16] or aggregation-caused quenching (ACQ).[17] Reports on luminescence-based sensing and a change of wavelength and colour usually relate to nanoparticles such as quantum dots, up-converting metal fluorides/oxides, MOFs, or carbon dots.[18]

Aiming at a luminescence detection based on a wavelength/colour-changing system, we recently showed inorganic–organic hybrid nanoparticles (IOH-NPs) such as $[La(OH)_2]^+[ARS]^-$ (ARS: alizarin red S)[19] or a mixture of $[La(OH)]^{2+}[ICG]^-{}_2$ and $[La(OH)]^{2+}{}_2[PTC]^{4-}$ (ICG: indocyanine green, PTC: perylene-3,4,9,10-tetracarboxylate).[20] Generally, these IOH-NPs are characterized by a fluorescent organic dye anion, which is combined with an inorganic cation to obtain an insoluble compound, and thus, nanoparticles in water. In detail, $[La(OH)_2]^+[ARS]^-$ IOH-NPs show a pH-dependent colour shift with green emission at pH 5.0–9.0 and red emission at pH < 4.5 and can be used to monitor the intracellular pH.[19] $[La(OH)]^{2+}[ICG]^-{}_2$ and $[La(OH)]^{2+}{}_2[PTC]^{4-}$ IOH-NPs allow to monitor the particle dissolution *in vitro* with red emission of

[a]*Karlsruhe Institute of Technology (KIT), Institute for Inorganic Chemistry, Engesserstrasse 15, 76131 Karlsruhe, Germany. E-mail: claus.feldmann@kit.edu*
[b]*Chair of Bioinorganic Chemistry, Heinrich-Heine-Universität Düsseldorf, Universitätsstraße 1, 40225 Düsseldorf, Germany*

† Electronic supplementary information (ESI) available: Details related to analytical equipment, characterization of $TREN\text{-}1,2\text{-}HOPO_3$, nanoparticle characterization of $(Eu^{3+}{}_4[PTC]^{4-}{}_3)_{0.9}(Eu^{3+}[TREN\text{-}1,2\text{-}HOPO]^{3-})_{0.1}$ and $Eu^{3+}{}_4[PTC]^{4-}{}_3$ as well as luminescence spectra. See DOI: https://doi.org/10.1039/d4dt02344g

the intact nanoparticles and green emission after their dissolution.[20] However, these IOH-NPs have the disadvantage of a broad and partially weak emission. Monitoring the dissolution, moreover, requires two different types of nanoparticles.

Experimental section

Synthesis

The starting materials perylene-3,4,9,10-tetracarboxylic dianhydride (PTCDA, abcr, 98%), $EuCl_3{\cdot}6\ H_2O$ (Sigma-Aldrich, 99.9%), NaOH (VWR, ≥98%), $HCl_{(aq)}$ (VWR, 37%), $NaHCO_3$ (VWR, 98%) and ethanol (Seulberger, 99%) were used as received. All solutions and suspensions were prepared with deionized (DI) water that was boiled 30 min, cooled and stored under nitrogen to remove and avoid dissolved CO_2.

TREN-1,2-HOPO was synthesized according to the literature (ESI: Fig. S1†).[21]

$(Eu^{3+}{}_4[PTC]^{4-}{}_3)_{0.78}(Eu^{3+}[TREN\text{-}1,2\text{-}HOPO]^{3-})_{0.22}$ IOH-NPs. 6.3 mg (0.016 mmol) of perylene-3,4,9,10-tetracarboxylic dianhydride (PTCDA, abcr, 98%) were dissolved in 25 mL of 10 mmol L^{-1} NaOH by heating to 60 °C (pH 10–11). After neutralisation with HCl (10 mmol L^{-1}) (pH 6.5–7.0), 15 mL of ethanol were added. Thereafter, a solution of 9.3 mg (0.025 mmol) $EuCl_3{\cdot}6\ H_2O$ (Sigma-Aldrich, 99.9%) and 0.8 mg TREN-1,2-HOPO (0.0015 mmol) dissolved in 0.5 mL of water were injected at 95 °C (oil bath) into the aforementioned PTCDA solution, which instantaneous resulted in the nucleation of nanoparticles. After cooling, the as-prepared $(Eu^{3+}{}_4[PTC]^{4-}{}_3)_{0.78}(Eu^{3+}[TREN\text{-}1,2\text{-}HOPO]^{3-})_{0.22}$ IOH-NPs were separated by centrifugation (10 000 rpm, 15 min) and purified twice by redispersion/centrifugation in/from water. Finally, aqueous suspensions or dried powder samples were obtained.

$Eu^{3+}{}_4[PTC]^{4-}{}_3$ IOH-NPs were prepared similar to the above $(Eu^{3+}{}_4[PTC]^{4-}{}_3)_{0.78}(Eu^{3+}[TREN\text{-}1,2\text{-}HOPO]^{3-})_{0.22}$ IOH-NPs without addition of TREN-1,2-HOPO.

Carbonate-initiated emission-colour-shift. First of all, a $NaHCO_3$ stock solution (4 mmol L^{-1}) was prepared by dissolution of 33.6 mg (0.40 mmol) $NaHCO_3$ in 100 mL of DI water. The DI water was boiled 30 min, cooled and stored under nitrogen to remove and avoid dissolved CO_2. Furthermore, the DI water was set to pH 6.5 prior to use. Based on the stock solution, further solutions with concentrations of 3, 2, 1, 0.2, 0.02 and 0.002 mM were obtained by dilution. Subsequently, 1 mL of the $(Eu^{3+}{}_4[PTC]^{4-}{}_3)_{0.78}(Eu^{3+}[TREN\text{-}1,2\text{-}HOPO]^{3-})_{0.22}$ IOH-NP suspension (0.5 mg mL^{-1}) was mixed with 1 mL of the above $NaHCO_3$ solutions resulting in suspensions with the specified 2, 1.5, 1, 0.5, 0.1, 0.01, 0.001 mM $NaHCO_3$ concentration.

In the case of pure DI water, 1 mL of DI water was mixed with the IOH-NP suspension instead of the aforementioned $NaHCO_3$ solutions. In the case of tap water, 0.5 mL of tap water and 0.5 mL of DI water were mixed with 1 mL of the IOH-NP suspension, resulting in a tap water dilution by a factor of 1 : 4.

Luminescence characterization was performed similar for all suspensions with recording excitation and emission spectra after equilibration with 15 min of thorough mixing. For the integration of the PTC-based green emission, the Eu^{3+}-based emission peak at 616 nm was omitted by interpolation of the PTC-based emission from 606 to 633 nm.

Analytical techniques

Details regarding analytical equipment, characterization of TREN-1,2-HOPO, nanoparticle characterization of $(Eu^{3+}{}_4[PTC]^{4-}{}_3)_{0.78}(Eu^{3+}[TREN\text{-}1,2\text{-}HOPO]^{3-})_{0.22}$ and $Eu^{3+}{}_4[PTC]^{4-}{}_3$ IOH-NPs, and luminescence spectra are described in the ESI.†

Results and discussion

Nanoparticle synthesis

Here, we here report on $(Eu^{3+}{}_4[PTC]^{4-}{}_3)_{0.78}(Eu^{3+}[TREN\text{-}1,2\text{-}HOPO]^{3-})_{0.22}$ IOH-NPs containing Eu^{3+}, tris[(1-hydroxy-2-oxo-1,2-dihydropyridine-6-carboxamido)ethyl]amine (TREN-1,2-HOPO) and perylene-3,4,9,10-tetracarboxylate (PTC) (Fig. 1). Herein, TREN-1,2-HOPO serves as an antenna ligand that guarantees an efficient emission of red light by Eu^{3+} even in water.[22] In contrast, the emission of PTC is completely quenched in the solid nanoparticles but results in intense green emission after its release into solution. As a result, $(Eu^{3+}{}_4[PTC]^{4-}{}_3)_{0.78}(Eu^{3+}[TREN\text{-}1,2\text{-}HOPO]^{3-})_{0.22}$ IOH-NPs show Eu^{3+}-based red emission and intense green emission after PTC release. Exemplarily, this effect can be used for qualitative and quantitative luminescence detection of carbonate in potable water.

$(Eu^{3+}{}_4[PTC]^{4-}{}_3)_{0.78}(Eu^{3+}[TREN\text{-}1,2\text{-}HOPO]^{3-})_{0.22}$ IOH-NPs are prepared *via* a simple aqueous synthesis. First of all, perylene-3,4,9,10-tetracarboxylic dianhydride (PTCDA) as the starting material needs to be converted into the water-soluble perylene-3,4,9,10-tetracarboxylate ($[PTC]^{4-}$) by treatment with aqueous NaOH at 60 °C. The underlying reaction can be easily followed by the insoluble red PTCDA changing to soluble yellow $[PTC]^{4-}$. After neutralization with HCl, ethanol was added (H_2O : EtOH = 60 : 40) to reduce the polarity of the solvent,

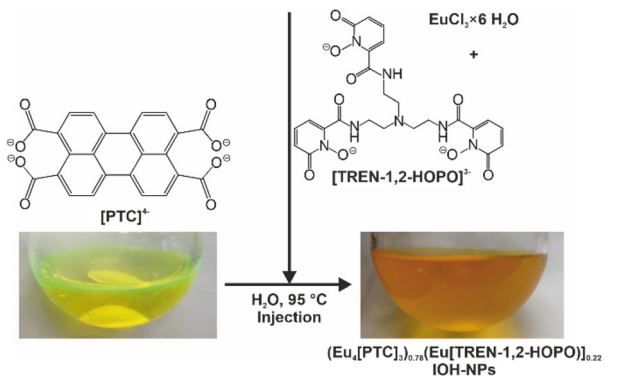

Fig. 1 Scheme of the synthesis of $(Eu^{3+}{}_4[PTC]^{4-}{}_3)_{0.78}(Eu^{3+}[TREN\text{-}1,2\text{-}HOPO]^{3-})_{0.22}$ IOH-NPs.

which supports the formation of smaller nanoparticles and more stable suspensions thereafter (Fig. 1). This also allows avoiding a reformation of insoluble PTCDA (at >60% of H_2O) as well as of insoluble Na_4(PTC) (at >40% of EtOH). In addition to the Na_4(PTC) solution, $EuCl_3{\cdot}6H_2O$ and H_3TREN-1,2-HOPO were dissolved in water. Thereafter, this second solution was injected into the Na_4(PTC) solution with vigorous stirring at 95 °C (Fig. 1). The nucleation of $(Eu^{3+}{}_4[PTC]^{4-}{}_3)_{0.78}(Eu^{3+}[TREN\text{-}1,2\text{-}HOPO]^{3-})_{0.22}$ IOH-NPs was indicated by the immediate formation of an orange suspension. The injection at elevated temperature promotes the nucleation of nanoparticles. Finally, the IOH-NPs were purified by centrifugation/redispersion from/in water.

Particle size and particle size distribution of the as-prepared $(Eu^{3+}{}_4[PTC]^{4-}{}_3)_{0.78}(Eu^{3+}[TREN\text{-}1,2\text{-}HOPO]^{3-})_{0.22}$ nanoparticles were evaluated based on scanning electron microscopy (SEM) and dynamic light scattering (DLS). SEM images show rod-shaped nanoparticles with a length of about 60 nm and a diameter of about 5 nm (Fig. 2b; and ESI Fig. S2†). Based on a statistical evaluation of >100 particles on SEM images, a mean rod length of 63 ± 8 nm was determined (Fig. 2a).[20] Such rod-like shape is to be expected due to PTC-based π-stacking. Due to the high-polarity and extensive hydrogen bridging, DLS analysis in water often results in very broad particle size distributions due to overlapping long-ranging water-adhesion layers. To this concern, the IOH-NPs were redispersed in diethylene glycol (DEG) as a colloidally stabilizing solvent.[23] In DEG, DLS resulted in a mean hydrodynamic particle diameter of 94 ± 7 nm (Fig. 2a; and ESI: Fig. S3†), which reflects the length of the rod-shaped IOH-NPs and which is in accordance with the results from SEM. In water, the as-prepared IOH-NPs exhibit a distinct negative surface charging with a zeta potential of −30 to −40 mV at pH = 6–9 (Fig. 2c), which is also the background of the good colloidal stability of aqueous suspensions (Fig. 2c and d).

In regard of the chemical composition of the $(Eu^{3+}{}_4[PTC]^{4-}{}_3)_{0.78}(Eu^{3+}[TREN\text{-}1,2\text{-}HOPO]^{3-})_{0.22}$ IOH-NPs, first of all, the presence of both Eu^{3+}, TREN-1,2-HOPO, and PTC is crucial and clearly evidenced by the luminescence features of the IOH-NPs (see Fig. 3 and 4). Thus, red emission of Eu^{3+} is

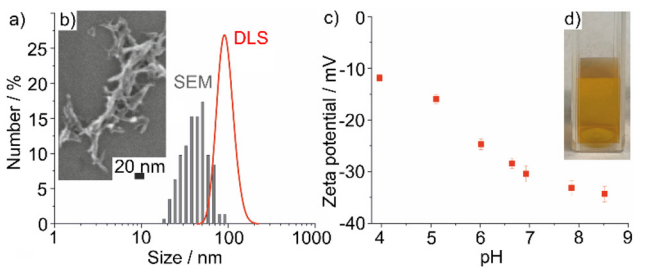

Fig. 2 Particle characterization of $(Eu^{3+}{}_4[PTC]^{4-}{}_3)_{0.78}(Eu^{3+}[TREN\text{-}1,2\text{-}HOPO]^{3-})_{0.22}$ IOH-NPs: (a) particle size and particle size distribution according to SEM (statistical evaluation of >100 nanoparticles) and DLS (in DEG); (b) SEM image; (c) zeta potential analysis (in water); (d) photo of the aqueous suspension (0.5 mg mL^{-1}).

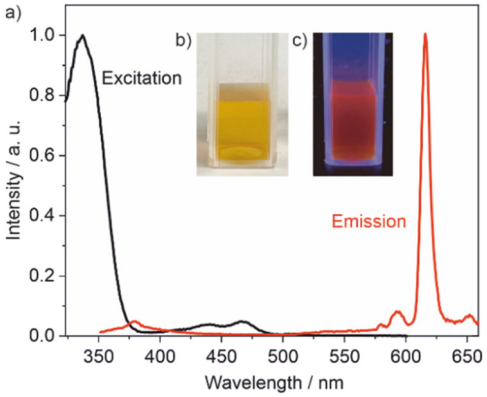

Fig. 3 Luminescence of $(Eu^{3+}{}_4[PTC]^{4-}{}_3)_{0.78}(Eu^{3+}[TREN\text{-}1,2\text{-}HOPO]^{3-})_{0.22}$ IOH-NPs (0.5 mg mL^{-1}, DI water): (a) excitation (λ_{em} = 616 nm) and emission (λ_{ex} = 337 nm) spectra; (b) photo of aqueous suspension (daylight); (c) photo of aqueous suspension (λ_{ex} = 365 nm).

observed in water only in the presence of TREN-1,2-HOPO as antenna, whereas the green emission after nanoparticle dissolution evidences the presence of PTC. For quantification, X-ray diffraction (XRD), Fourier-transform infrared (FT-IR) spectroscopy, total organics combustion with thermogravimetry (TG), and elemental analysis (EA) were applied. XRD indicates the IOH-NPs to be non-crystalline (ESI: Fig. S4†), which is not a surprise taking a synthesis at moderate temperature in water into account. According to FT-IR (ESI: Tables S1, S2; and Fig. S5†), all vibrations of $(Eu^{3+}{}_4[PTC]^{4-}{}_3)_{0.78}(Eu^{3+}[TREN\text{-}1,2\text{-}HOPO]^{3-})_{0.22}$ can be attributed to TREN-1,2-HOPO (especially: ν(C═O): 1680, ν(C–N): 1207 cm^{-1}) and PTC (specifically: ν(C═O): 1595 cm^{-1}). Moreover, the broad band at 3650–3100 cm^{-1} shows the presence of H_2O ν(O–H).

TG shows a three-step decomposition with a total mass loss of 63.3 wt% up to 600 °C (ESI: Fig. S6a†), whereof the first step (5.4 wt%, <200 °C) relates to adsorbed water. After correction for this adsorbed water, the total organics combustion amounts to 67.1 wt%. The thermal residue was identified by XRD to be Eu_2O_3, which indicates total-organics combustion after heating to 1200 °C (ESI: Fig. S6b†). EA reveals C/H/N contents of 42.9 wt% C, 2.2 wt% H and 1.2 wt% N, which, after correction for 5.4 wt% of adsorbed water, results in 45.5 wt% C, 1.7 wt% H and 1.3 wt% N. As only TREN-1,2-HOPO contains nitrogen, the PTC-to-TREN-1,2-HOPO ratio can be deduced to 10.7, which reflects the as-used 10 : 1 ratio of the starting materials. With this information, the IOH-NPs can be assumed to contain 25% $Eu^{3+}[TREN\text{-}1,2\text{-}HOPO]^{3-}$ and 75% $Eu^{3+}{}_4[PTC]^{4-}{}_3$ (*composition of* $Eu^{3+}{}_4[PTC]^{4-}{}_3$ *in* ESI: Fig. S7†). With the assumed composition, values of 45.3 wt% C, 1.7 wt% H, 1.4 wt% N and a total organics combustion of 67.1 wt% are calculated that agree with the experimental data. Based on TG and XRD showing a solid remnant of 31.3% Eu_2O_3 (corrected for 5.4% of adsorbed water: 33.2% Eu_2O_3 or 28.8% Eu), finally, the Eu^{3+} content of the IOH-NPs can be obtained (calcd: 28.7% Eu). In sum, this confirms the composition $(Eu^{3+}{}_4[PTC]^{4-}{}_3)_{0.78}(Eu^{3+}[TREN\text{-}1,2\text{-}HOPO]^{3-})_{0.22}$ of the IOH-NPs.

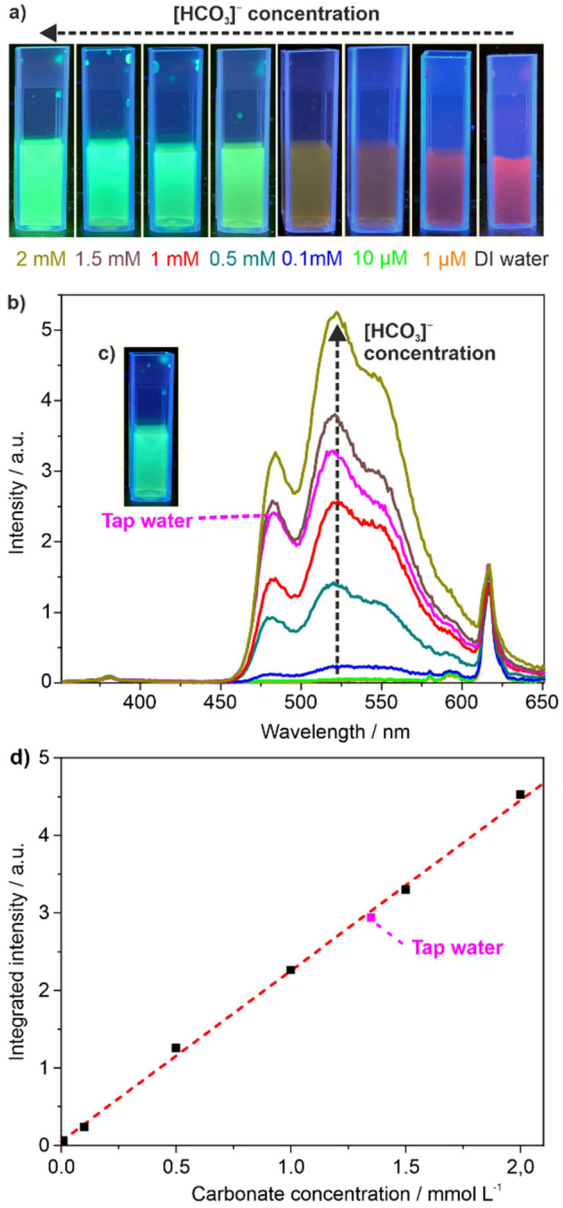

Fig. 4 Luminescence of $(Eu^{3+}{}_4[PTC]^{4-}{}_3)_{0.78}(Eu^{3+}[TREN\text{-}1,2\text{-}HOPO]^{3-})_{0.22}$ IOH-NPs (0.25 mg mL^{-1}, water) at different carbonate concentrations: (a) photos of aqueous suspensions (1 µM, 10 µM, 0.1 mM, 0.5 mM, 1 mM, 1.5 mM, 2 mM $NaHCO_3$, λ_{ex} = 365 nm); (b) emission spectra (1 µM, 10 µM, 0.1 mM, 0.5 mM, 1 mM, 1.5 mM, 2 mM $NaHCO_3$, λ_{ex} = 337 nm); (c) photo of aqueous suspension with tap water; (d) correlation of carbonate concentration (1 µM to 2 mM, black squares) and intensity of green emission extracted from spectra in (b) with the result for local tap water (pink square).

Luminescence properties

In regard of the luminescence of the $(Eu^{3+}{}_4[PTC]^{4-}{}_3)_{0.78}(Eu^{3+}[TREN\text{-}1,2\text{-}HOPO]^{3-})_{0.22}$ IOH-NPs, the red emission of the as-prepared aqueous suspensions can be even seen with the naked eye upon excitation at 310–370 nm (UV lamp or UV-LED, Fig. 3). The luminescence characteristics of the $(Eu^{3+}{}_4[PTC]^{4-}{}_3)_{0.78}(Eu^{3+}[TREN\text{-}1,2\text{-}HOPO]^{3-})_{0.22}$ IOH-NPs are very similar to aqueous solutions of the [Eu(TREN-1,2-HOPO)(H_2O)] complex and can be assigned to the well-known Eu^{3+}-based emission with its maximum at 616 nm due to $^5D_0 \rightarrow {}^7F_2$ transition. Moreover, the broad absorption below 380 nm originates from the TREN-1,2-HOPO ligand (Fig. 3; and ESI: Fig. S8†). In sum, TREN-1,2-HOPO serves as efficient antenna ligand for Eu^{3+}, which does not show any notable emission in water in absence of TREN-1,2-HOPO.

In regard of PTC, the $(Eu^{3+}{}_4[PTC]^{4-}{}_3)_{0.78}(Eu^{3+}[TREN\text{-}1,2\text{-}HOPO]^{3-})_{0.22}$ IOH-NPs do not show any emission due to aggregation-caused quenching (ACQ) and the π-stacking of the PTC molecules in the solid state (Fig. 3).[17,20] Because of the low amount of TREN-1,2-HOPO in the $(Eu^{3+}{}_4[PTC]^{4-}{}_3)_{0.78}(Eu^{3+}[TREN\text{-}1,2\text{-}HOPO]^{3-})_{0.22}$ IOH-NPs, π-stacking and quenching of PTC are also not disturbed. A solution of $Na_4(PTC)$ in water, in contrast, shows strong absorption at 280–380 nm and intense green emission at 480–620 nm (ESI: Fig. S9†).

With the intention of a trigger-initiated emission-colour shift, we monitored the dissolution of the IOH-NPs, aiming at a different emission of the intact solid nanoparticles and after their dissolution in water. In this regard, $(Eu^{3+}{}_4[PTC]^{4-}{}_3)_{0.78}(Eu^{3+}[TREN\text{-}1,2\text{-}HOPO]^{3-})_{0.22}$ IOH-NPs are stable in deionized (DI) water (pH 5 to 7, room temperature). A dissolution of the $(Eu^{3+}{}_4[PTC]^{4-}{}_3)_{0.78}(Eu^{3+}[TREN\text{-}1,2\text{-}HOPO]^{3-})_{0.22}$ IOH-NPs, however, can be initiated by addition of carbonate (Fig. 4a). After addition of certain amounts of $NaHCO_3$ (*i.e.*, 1 µM, 10 µM, 0.1 mM, 0.5 mM, 1 mM, 1.5 mM, 2 mM), the emission clearly shifts from red to green. This observation can be explained by the intact, solid IOH-NPs, which show Eu^{3+}-based red emission. Upon addition of $NaHCO_3$, however, $[PTC]^{4-}$ is released from the $(Eu^{3+}{}_4[PTC]^{4-}{}_3)_{0.78}(Eu^{3+}[TREN\text{-}1,2\text{-}HOPO]^{3-})_{0.22}$ IOH-NPs into solution, where its luminescence is not quenched, and therefore, shows intense green emission. Thus, the carbonate-initiated emission-colour shift is driven by a stronger coordination of carbonate to Eu^{3+} than of the carboxylate PTC according to the following reaction: $(Eu^{3+}{}_4[PTC]^{4-}{}_3)_{0.78}(Eu^{3+}[TREN\text{-}1,2\text{-}HOPO]^{3-})_{0.22} + 4x\ [HCO_3]^- \rightarrow (Eu_4[(PTC)_{1-x}(HCO_3)_{4x}]_3)_{0.78}(Eu[TREN\text{-}1,2\text{-}HOPO])_{0.22} + x\ [PTC]^{4-}$. A comparable ligand exchange was also described for molecular coordination complexes[24] but was not yet shown for nanoparticles. In total, the emission colour changes from red to green and, depending on the respective $NaHCO_3$ concentration, including all mixed colours in between due to additive colour mixing (Fig. 4a).

The correlation between the intensity of the PTC-driven green emission and the $NaHCO_3$ concentration is also clearly visible when recording the respective emission spectra (Fig. 4b; and ESI: Fig. S10†). Whereas the green emission is weak for 100 nM and 1 µM $NaHCO_3$, starting at 10 µM, the green emission increases significantly and is also visible with the naked eye (Fig. 4a). In contrast to the concentration-dependent green emission of PTC, the Eu^{3+}-based red emission at 616 nm is more-or-less constant and independent of the $NaHCO_3$ concentration (Fig. 4b). As a test with certain practical relevance, we have treated local tap water with $(Eu^{3+}{}_4[PTC]^{4-}{}_3)_{0.78}(Eu^{3+}[TREN\text{-}1,2\text{-}HOPO]^{3-})_{0.22}$ IOH-NPs. The

presence of carbonate is again indicated by the occurring green emission (Fig. 4b).

Although the current experiments were more performed to prove a trigger-initiated emission-colour shift of a new type of nanoparticles in general then to allow a quantification, the carbonate concentration and the intensity of the green emission (extracted from spectra in Fig. 4b) already show a surprisingly good linear correlation (Fig. 4d). Even a luminescence-based analysis of the carbonate concentration of local tap water is possible (Fig. 4d). Thus, a concentration of 1.31 mM was determined based on the intensity of the green emission in suspension. After correction for the dilution of the tap water by a factor 1 : 4 during sample preparation (see Experimental section), the result of 5.24 mM carbonate obtained from the emission intensity is in agreement with data given by the local water authority (average carbonate concentration: 333 mg L^{-1}, 5.3 mM).[25]

With a current detection limit of 1 μM to 2 mM (Fig. 4), the $(Eu^{3+}{}_4[PTC]^{4-}{}_3)_{0.78}(Eu^{3+}[TREN\text{-}1,2\text{-}HOPO]^{3-})_{0.22}$ IOH-NP-based carbonate detection is possible in a similar concentration range as with comparable luminescence-based systems for carbonate detection, such as molecular coordination complexes or MOFs (1 μM–25 mM).[24,26] For the reliability of the carbonate-initiated emission-colour shift for future quantitative analysis, furthermore, potential limitations need to be addressed. First of all, the pH is relevant. To this concern, suspensions need to exhibit a pH of 5–7. In this pH range, the effect of the pH only (without any carbonate addition) on the emission is low in comparison to the carbonate-initiated emission increase (Fig. 4b; and ESI: Fig. S11a†). Here, the linear correlation between emission and carbonate concentration also confirms any significant additional effect of the pH (Fig. 4d). At pH > 7, however, $Eu(OH)_3$ can be formed, which also leads to a release of PTC, and thus, an increase of green emission (ESI: Fig. S11b†). At pH < 5, the emission is less affected by the pH but PTCDA starts to precipitate, which is visibly indicated by its red colour. A similar shift of the emission colour can be also expected from species with similar ligand properties as carbonate, such as organic carboxylates or phosphate. For the latter, the effect on the emission of the IOH-NPs is already shown (ESI: Fig. S12†) and can be ascribed to the following reaction: $(Eu^{3+}{}_4[PTC]^{4-}{}_3)_{0.78}(Eu^{3+}[TREN\text{-}1,2\text{-}HOPO]^{3-})_{0.22} + 2x\,[HPO_4]^{2-} \rightarrow (Eu_4[(PTC)_{1-x}(HPO_4)_{2x}]_3)_{0.78}(Eu[TREN\text{-}1,2\text{-}HOPO])_{0.22} + x[PTC]^{4-}$. In sum, the carbonate-initiated emission-colour shift of the $(Eu^{3+}{}_4[PTC]^{4-}{}_3)_{0.78}(Eu^{3+}[TREN\text{-}1,2\text{-}HOPO]^{3-})_{0.22}$ IOH-NPs could already be relevant for qualitative and/or quantitative detection in potable water.

Conclusions and outlook

In conclusion, $(Eu^{3+}{}_4[PTC]^{4-}{}_3)_{0.78}(Eu^{3+}[TREN\text{-}1,2\text{-}HOPO]^{3-})_{0.22}$ inorganic–organic hybrid nanoparticles (IOH-NPs) are prepared in water and contain Eu^{3+}, tris[(1-hydroxy-2-oxo-1,2-dihydropyridine-6-carboxamido)-ethyl]amine (TREN-1,2-HOPO) and perylene-3,4,9,10-tetracarboxylate (PTC). The rod-shaped IOH-NPs are colloidally stable in water and exhibit a length of about 60 nm and a diameter of about 5 nm. TREN-1,2-HOPO serves as antenna and guarantes for intense Eu^{3+}-based red emission of the IOH-NPs in water. The luminescence of PTC is quenched in the solid nanoparticles due to aggregation-caused quenching. After dissolution of the IOH-NPs, however, the released free PTC shows intense green emission. This red-green emission-colour-shift can be initiated by carbonate as a trigger. Surprisingly, the effect not only allows a qualitative indication but also a quantitative correlation of the intensity of the green emission and the carbonate concentration. This was validated for the carbonate concentration of local tap water. The carbonate-initiated emission-colour-shift of $(Eu^{3+}{}_4[PTC]^{4-}{}_3)_{0.78}(Eu^{3+}[TREN\text{-}1,2\text{-}HOPO]^{3-})_{0.22}$ IOH-NPs is first shown and may allow an easy detection of carbonate, for instance in tap or potable water. A potential ratiometric luminescence sensing based on the IOH-NPs will require a further evaluation regarding selectivity and concentration ranges.

Data availability

Additional data regarding experiments and methods can be obtained from the ESI† and on request from the authors.

Conflicts of interest

There are no conflicts to declare.

Acknowledgements

The authors acknowledge financial support from the Deutsche Forschungsgemeinschaft (DFG) through the Collaborative Research Center “4f for Future” (CRC 1573, project number 471424360), project C4. Furthermore, C. R. is grateful to the Studienstiftung des Deutschen Volkes for scholarship. Finally, L. J. D. thanks Dr Henning Widmann for synthesizing a batch of TREN-1,2-HOPO.

References

1 (*a*) D. Wu, A. C. Sedgwick, T. Gunnlaugsson, E. U. Akkaya, J. Yoon and T. D. James, *Chem. Soc. Rev.*, 2017, **46**, 7105–7123; (*b*) M. I. Stich, L. H. Fischer and O. S. Wolfbeis, *Chem. Soc. Rev.*, 2010, **39**, 3102–3114.

2 (*a*) J. J. Zhang, F. F. Cheng, J. J. Li, J.-J. Zhu and Y. Lu, *Nano Today*, 2016, **11**, 309–329; (*b*) M. H. Lee, J. S. Kim and J. L. Sessler, *Chem. Soc. Rev.*, 2015, **44**, 4185–4191.

3 (*a*) L. Wang, M. S. Frei, A. Salim and K. Johnsson, *J. Am. Chem. Soc.*, 2019, **141**, 2770–2781; (*b*) O. S. Wolfbeis, *Chem. Soc. Rev.*, 2015, **44**, 4743–4768.

4 (*a*) M. Gao, F. Yu, C. Lv, J. Choo and L. Chen, *Chem. Soc. Rev.*, 2017, **46**, 2237–2271; (*b*) S. Kunjachan, J. Ehling,

G. Storm, F. Kiessling and T. Lammers, *Chem. Rev.*, 2015, **115**, 10907–10937.

5 (*a*) S.-H. Park, N. Kwon, J.-H. Lee, J. Yoon and I. Shin, *Chem. Soc. Rev.*, 2020, **49**, 143–179; (*b*) L. Chen, D. Liu, J. Peng, Q. Du and H. He, *Coord. Chem. Rev.*, 2020, **404**, 213113; (*c*) M. H. Lee, J. S. Kim and J. L. Sessler, *Chem. Soc. Rev.*, 2015, **44**, 4185–4191.

6 (*a*) J. Li, J. Xu, W. Guo, W. Zhong, Q. Li, L. Tan and L. Shang, *Sens. Actuators, B*, 2020, **305**, 127422; (*b*) X. Wang, S. Yu, W. Liu, L. Fu, Y. Wang, J. Li and L. Chen, *ACS Sens.*, 2018, **3**, 378–385; (*c*) W. Liu, X. Wang, Y. Wang, J. Li, D. Shen, Q. Kang and L. Chen, *Sens. Actuators, B*, 2018, **262**, 810–817; (*d*) A. Zhu, Q. Qu, X. Shao, B. Kong and Y. Tian, *Angew. Chem., Int. Ed.*, 2012, **51**, 7185–7189.

7 (*a*) A. V. Orlova, N. V. Shmychov, K. Y. Vlasova, T. M. Iakimova, L. S. Lepnev, A. A. Eliseev and V. V. Utochnikova, *Dalton Trans.*, 2024, **53**, 3980–3964; (*b*) L. Chen, D. Li, J. Peng, Q. Du and H. He, *Coord. Chem. Rev.*, 2020, **404**, 213113; (*c*) Z. Zhang, Q. Han, J. W. Lau and B. Xing, *ACS Mater. Lett.*, 2020, **2**, 1516–1531; (*d*) R. Gui, X. Fang and D. Yan, *J. Mater. Chem. C*, 2019, **7**, 3399–3412.

8 M. L. Aulsebrook, B. Graham, M. R. Grace and K. L. Tuck, *Tetrahedron*, 2014, **70**, 4367–4372.

9 Y.-W. Yip, G.-L. Law and W.-T. Wong, *Dalton Trans.*, 2016, **45**, 928–935.

10 T. M. Wickramaratne and V. C. Pierre, *Bioconjugate Chem.*, 2015, **26**, 63–70.

11 T. Liu, A. Nonat, M. Beyler, M. Regueiro-Figueroa, K. N. Nono, O. Jeannin, F. Camerel, F. Debaene, S. Cianférani-Sanglier, R. Tripier, C. Platas-Iglesias and L. J. Charbonnière, *Angew. Chem., Int. Ed.*, 2014, **53**, 7259–7263.

12 J. Sahoo, R. Arunachalam, P. S. Subramanian, E. Suresh, A. Valkonen, K. Rissanen and M. Albrecht, *Angew. Chem., Int. Ed.*, 2016, **55**, 9625–9629.

13 Y. Bretonnière, M. J. Cann, D. Parker and R. Slater, *Chem. Commun.*, 2002, 1930–1931.

14 R. Pal, D. Parker and L. C. Costello, *Org. Biomol. Chem.*, 2009, **7**, 1525–1528.

15 C. Ronda, *Luminescence*, Wiley-VCH, Weinheim, 2007.

16 (*a*) M. Li, T. Chen, J. J. Gooding and J. Liu, *ACS Sens.*, 2019, **4**, 1732–1748; (*b*) A. L. Efros and L. E. Brus, *ACS Nano*, 2021, **15**, 6192–6210.

17 H. Wang, M. Ai and J. Liu, *Anal. Bioanal. Chem.*, 2023, **415**, 2185–2191.

18 (*a*) X. Zhai, P. Feng, N. Song, G. Zhao, Q. Liu, L. Liu, M. Tang and Y. Tang, *Inorg. Chem. Front.*, 2022, **9**, 1406–1415; (*b*) C. Wang, H. Lin, X. Ge, J. Mu, L. Su, X. Zhang, M. Niu, H. Yang and J. Song, *Adv. Funct. Mater.*, 2021, **31**, 2009942; (*c*) M. Jia, Z. Sun, M. Zhang, H. Xu and Z. Fu, *Nanoscale*, 2020, **12**, 20776–20785; (*d*) R. Jalili, A. Khataee, M.-R. Rashidi and R. Luque, *Sens. Actuators, B*, 2019, **297**, 126775; (*e*) N. Fahimi-Kashani and M. R. Hormozi-Nezhad, *Sens. Actuators, B*, 2020, **332**, 128580.

19 K. Sabljo, J. Napp, F. Alves and C. Feldmann, *Chem. Commun.*, 2022, **58**, 9417–9420.

20 C. Ritschel, J. Napp, F. Alves and C. Feldmann, *Nanoscale*, 2022, **14**, 16249–16255.

21 J. Xu, D. G. Churchill, M. Botta and K. N. Raymond, *Inorg. Chem.*, 2004, **43**, 5492–5494.

22 (*a*) S.-Y. Huang and V. C. Pierre, *Chem. Commun.*, 2018, **54**, 9210–9213; (*b*) C. J. Jocher, E. G. Moore, J. Xu, S. Avedano, M. Botta, S. Aime and K. N. Raymond, *Inorg. Chem.*, 2007, **46**, 9182–9191.

23 H. Dong, Y.-C. Chen and C. Feldmann, *Green Chem.*, 2015, **17**, 4107–4132.

24 S. J. Butler and D. Parker, *Chem. Soc. Rev.*, 2013, **42**, 1652–1666.

25 **https://www.stadtwerke-karlsruhe.de**: Trinkwasser-Jahresmittelwerte-KA.pdf (access on May 15th, 2024).

26 (*a*) L. Peng, W. Guo, N. Wu, Y. Liu, M. Wang, B. Liu, J. Tian, X. Wei and W. Yang, *Spectrochim. Acta, Part A*, 2023, **299**, 122844; (*b*) W. Wang, F. Zhao, M. Li, C. Zhang, Y. Shao and Y. Tian, *Angew. Chem., Int. Ed.*, 2019, **58**, 5256–5260.

